JOURNAL OF MATERIALS SCIENCE 18 (1983) 637–651

Review
Calcination of precipitated $Mg(OH)_2$ to active MgO in the production of refractory and chemical grade MgO

J. GREEN
Mineral Products Department, Billiton Research BV, Arnhem, The Netherlands

The processes that occur during the calcination of seawater or brine precipitated $Mg(OH)_2$ to active MgO are reviewed. Details of the commercial calcination of $Mg(OH)_2$, and of the crystallography, mechanism and kinetics of the thermal decomposition of $Mg(OH)_2$ to MgO are given. The effects of calcination conditions, and of chemical and physical properties of the $Mg(OH)_2$ on the properties of the active MgO product are discussed together with the influence of typical impurities in commercial products.

1. Introduction

The proportion of magnesia (MgO) produced from $Mg(OH)_2$ precipitated from magnesium-containing solutions (seawater, brine) has grown from zero in the 1930's to the present level of about 45% of the western world's installed MgO capacity of 6.5 Tg per annum. Some 75% of the $Mg(OH)_2$ produced in this way is used for the manufacture of refractory grade (and to a lesser extent chemical grade) MgO.

With the more widespread use of new steelmaking processes in the 1960's (e.g. the Linz–Donawitz converter), refractory grade MgO of very high chemical purity and close proximity to theoretical density was required by the refractories industry. This demand led to the introduction of the process shown in Fig. 1. To achieve adequate densification of the MgO, the process involves a three step procedure for the conversion of $Mg(OH)_2$ to refractory grade MgO. An important step in this process is the calcination of $Mg(OH)_2$ at low temperatures (700 to 1000° C) to a reactive MgO powder, which is then either briquetted before firing at high temperature (about 1900° C) to give a refractory grade MgO, or used as a raw material for magnesium chemical production.

The calcination of $Mg(OH)_2$ to MgO involves initial thermal decomposition of the $Mg(OH)_2$ at about 300° C:

$$Mg(OH)_2 \rightarrow MgO + H_2O. \quad (1)$$

As the temperature increases further, the following sequence of events occurs:

(a) Sudden recrystallization of MgO of normal cubic structure from a defective hydroxide layer of hexagonal structure. (Both the defect hydroxide and the MgO initially formed have abnormal unit cell dimensions.)

(b) Cracking of the precursor/product crystal into small fragments as the crystal fracture stress is exceeded.

(c) Gradual desorption of water trapped in the crystal agglomerate.

(d) Shrinkage of the MgO crystal lattice until the equilibrium unit cell dimension is reached.

(e) Growth of the MgO crystals caused by diffusional material transport.

(f) Sintering together of the MgO crystals.

These processes influence the properties of the MgO very strongly, but the extent to which they occur is a complex function of calcining temperature, time, atmosphere, impurity level in the material and $Mg(OH)_2$ morphology. Thus, a number of variables can have a significant bearing on the performance and economics of the calcining process, and on product quality. In this light, we review the crystallography, mechanism and kinetics of the thermal decomposition of $Mg(OH)_2$

0022–2461/83/030637–15$04–30/0

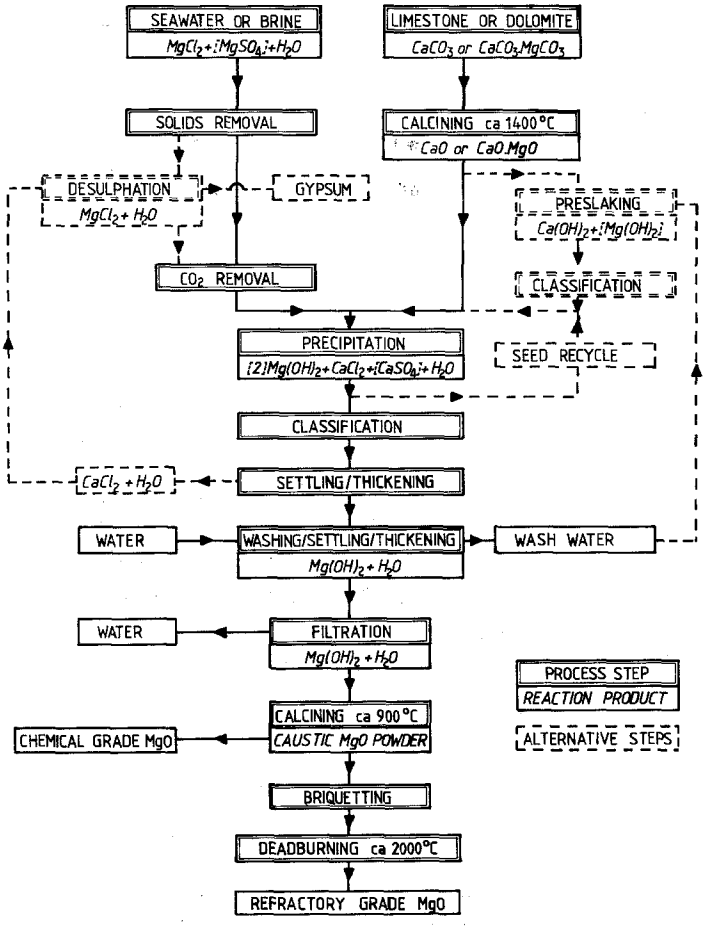

Figure 1 Flowscheme for the production of high quality chemical and refractory grade MgO from seawater or $MgCl_2$ brine.

to MgO, and look at factors affecting the properties of the product MgO.

2. Commercial calcination

In commercial plants the $Mg(OH)_2$ enters the calcining furnace (normally either a rotary kiln, or, in more modern plants, a Hereshoff or multiple-hearth kiln) as a slurry containing about 30 to 50 wt% water. In rotary kilns, the material is forced to move axially by kiln rotation, whereas in multi-hearth kilns a slowly turning rake (or rabble) ensures radial movement in a zigzag pattern to consecutively lower hearths via ports in the floor of each of the hearths. Simultaneously, hot gases from oil–air or gas–air burners (in multi-hearth kilns, fitted to each hearth; in rotary kilns, a single burner located in the firing zone) pass over and through the material. In multi-hearth kilns, the temperature of each hearth is monitored using thermocouples inserted into the gas space and the maximum temperature of about 1000° C is normally achieved in the hearths slightly below the middle of the kiln.

Dust entrained with the rising or exhaust gases is removed by e.g. an electroprecipitator before venting the gases. It is then recycled to the kiln either with the normal feed or to the perimeter of one of the lower hearths, which operate at higher temperatures than the gas exhaust. In such hearths, the material moves radially towards the rake shaft, thus avoiding short circuiting of the material flow to the next lower hearth. The amount of dust which is recycled may, in the extreme, amount to about 50% of the total MgO equivalent entering the kiln per time interval and consists of a mixture of $Mg(OH)_2$, partially decomposed material and fine MgO. The dust typically has a loss on ignition of about 10 wt% as compared with 31.5 wt% for $Mg(OH)_2$.

Active MgO is normally removed from the rotary kiln outlet or from the circumference of the lowest hearth by a screw conveyor at a temperature of 200 to 600° C. It typically has a loss on ignition of 1.5 wt%. This material is then passed by screw conveyors to further processing steps. MgO of 96% purity and, in refractory grades, with

densities > 94% of the theoretical can be obtained by the above procedure.

3. The thermal decomposition of $Mg(OH)_2$ to MgO

Brucite ($Mg(OH)_2$) is a member of the group of minerals known as the layer hydroxides whose structures show similarities to the layer and chain silicates. The thermal decomposition processes occurring in this simple class of compounds have been thoroughly investigated using a wide variety of techniques, and the results to 1970 have been reviewed by Brett *et al.* [1].

3.1. The crystallography of the decomposition reaction

The degrees of orientation which are found in practice between the crystal structure of the starting material (precursor) and that of its thermal decomposition product are extremely variable, continuously ranging from epitaxy (two-dimensional correspondence) to topotaxy (three-dimensional correspondence) [2].

The reaction of brucite to periclase (MgO) occurs with a very high degree of topotaxy, the hexagonal close packed structure of O^{2-} ions rearranging to a cubic close packed structure (see Fig. 2). The orientated crystallographic structure relationships of precursor and product are maintained during the reaction [3–13], as is the microscopic structure of the materials. Thus the hexagonal platelet structure of the brucite is retained in the $Mg(OH)_2$ to MgO reaction sequence [14].

3.2. The mechanism of the decomposition reaction

The step following from a knowledge of the structure of the parent and product of a decomposition reaction and their relationships is the obvious one of postulating a reaction mechanism. Two different models for the decomposition process have resulted from investigations of the dehydroxylation of brucite. The Goodman [15] model assumes that water is lost in a similar manner from all regions of the crystal with OH^- groups from adjacent layers combining to form water which diffuses away. Only minor length

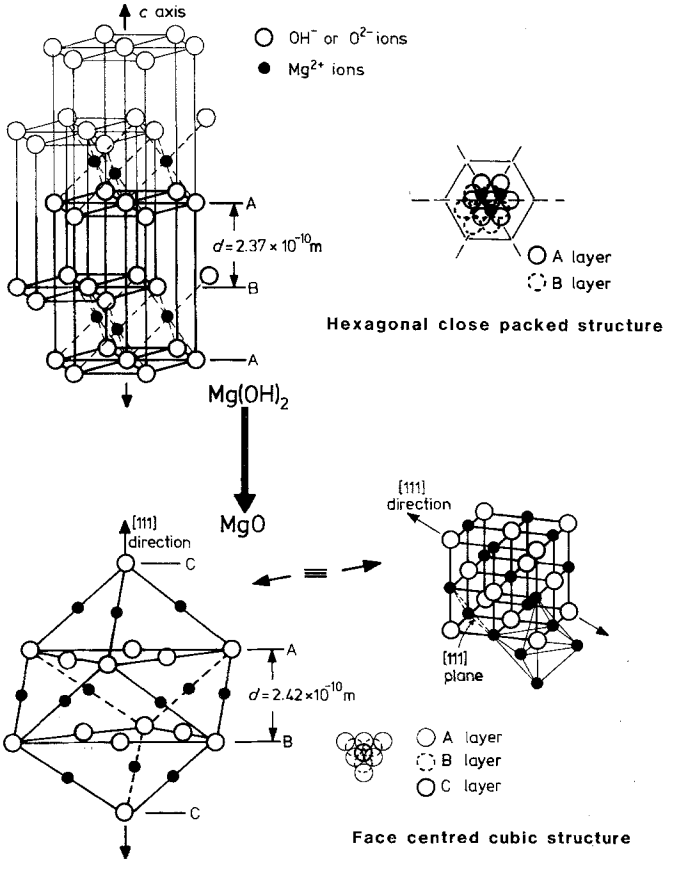

Figure 2 Crystallographic relationships in and between $Mg(OH)_2$ and MgO (after Brindley [19]).

reduction occurs in the basal (a–b) plane and the main shrinkage takes place along the c-axis. The reaction has thus been visualised as a chemical condensation between the OH^- groups on the upper surface of each brucite layer and those on the lower surface of the next. The reaction appears, from kinetic and optical microscope studies [16], to commence at an internal surface and advance towards the centre of the crystal. Such a mechanism could be described as homogeneous, and the structural transformation associated with the reaction has been recently interpreted [17, 18] in terms of a shear transformation requiring only reordering of the Mg^{2+} and O^{2-} ions without any long range diffusion of ions.

Ball and Taylor [3] and Brindley [19] independently proposed a second model known as the inhomogeneous mechanism. The reaction was assumed to occur simultaneously throughout the bulk of the crystal, this then developing "donor" and "acceptor" regions [3] during the decomposition process. Mg^{2+} ions were postulated to migrate from the donor to the acceptor regions with a counter migration of protons. The MgO crystals are formed from the acceptor regions, while OH^- ions combine with protons to form water molecules, which escape from the donor regions to leave behind intercrystalline pores.

There are two main attractions to the above inhomogeneous mechanism. Firstly, if cations and protons rather than H_2O molecules were the migrating species, less rearrangement of the structure would be expected and topotaxy would be more easily explained (hence the appeal of the transformational shear mechanism of Niepce *et al.* [17, 18] as applied to the homogeneous mechanism). Secondly, the creation of donor and acceptor regions in the brucite lattice explains the formation of a porous decomposition product. However, the inhomogeneous model is weak because it requires an *ad hoc* postulation of donor and acceptor regions, which requires, as corollary, the counter migration of two positively charged ions.

The original basis for the postulate of an inhomogeneous mechanism for the decomposition of brucite was not only the observed topotaxy and porous product, but also a reported intermediate phase [3, 7, 20–22]. In some cases "spinel-like" reflections were detected in X-ray powder and single crystal photographs of brucite crystals which had been decomposed at 800° C [3]. The presence of a spinel [20] or defect structure [21, 23–26] has been postulated to explain observations of an expanded lattice structure [22, 27–29] in other X-ray photographs of MgO formed by low temperature decomposition of brucite. The observation of spinel intermediates would indicate the Mg^{2+} ions to be tetrahedrally coordinated and thus to be migrating. However, this observation has been shown to derive from the presence of impurities in the brucite [30] since pure samples of $Mg(OH)_2$ did not show these reflections on decomposition. The experimental evidence for the inhomogeneous mechanism was thus invalidated.

An intermediate hexagonal phase has also been experimentally reported by other workers [22, 31] (and the theoretical basis for this derived [23, 25]), but an electron/optical microscope study by Gordon and Kingery [32, 33] led to its rejection. The decomposition process was evaluated as a nucleation and growth process with MgO nuclei forming coherently with the brucite matrix. Pampuch [34] gave a similar interpretation and considered that an intermediate stage of hybrid crystals leads on to the formation of new phases in topotactic decomposition reactions, while Freund *et al.* [23, 24] similarly postulated the formation of a defect layer of hydroxide structure but contracted unit cell dimensions, which suddenly recrystallizes to the cubic MgO structure as the fracture stress is exceeded in the defect layer [24, 35–38]. The MgO crystals formed have been shown [13, 22, 27–29, 32, 39–42] to have an expanded cubic lattice, which gradually decreases in size with increasing calcination temperature until the equilibrium unit cell dimension is achieved.

For brucite of large crystal size, this sudden recrystallization leads to cracking of the precursor/product crystal and hence to the formation of MgO crystals with a size of 5 to 10 nm [16, 38]. In polycrystalline (i.e. small crystal, 10 to 60 nm) precursor material, smaller values of strain have been observed [38] and complete reaction appears to be possible without cracking. Most commercially precipitated brucites have crystal sizes above this value so that cracking may be expected.

Observations made using mass spectrometry [36] and thermosonimetry [37] have apparently confirmed the stepwise decomposition of brucite to MgO consistent with the above cracking model. In this model, the evolution of water would be

slowed down as the defect layer builds to form a diffusion barrier, and speeded up as cracking caused by recrystallization occurs. The mechanism of decomposition leads to a hydrogen bond model for the dissociation of ionic hydroxides [43, 44]. Observed [44] broadening of the infrared spectrum O–H band at just below 300° C in brucite was interpreted as the start of OH–OH interaction at the crystal surfaces. A tunnelling mechanism of proton transfer was proposed [45] between adjacent OH^- groups, the resulting water molecules being removed by diffusion. At low temperatures, when the energy levels of the two adjacent OH^- groups overlap, tunnelling can take place, but at higher temperatures, where the OH^- groups are more widely spaced, proton jumping leads to the removal of OH^- groups with the loss of hydrogen [26, 46, 47]. The advancing interface concept [15] rather than the inhomogeneous mechanism is consistent with this interpretation of the dehydroxylation process, since proton tunnelling satisfactorily explains the reaction of OH^- groups in adjacent layers [15, 16]. Additionally, electrical neutrality is preserved so that the postulate of cation counter migration is no longer required.

Quantitative measurements [47] on hydrogen evolution during the decomposition process (showing two peaks, at 450° C and 750° C), indicate that about 0.5% of all the OH^- groups present in the starting $Mg(OH)_2$ yield hydrogen as gaseous species, i.e. 1000 kg of $Mg(OH)_2$ will give rise to more than $1\,m^3$ of hydrogen at $10^5\ Nm^{-2}$. Although the mechanism of hydrogen formation has been ascribed to an impurity oxidation reaction [48] (e.g. $Fe^{2+} + H_2O \rightleftharpoons Fe^{3+} + OH^- + \frac{1}{2}H_2$), this was rejected because of the low transition metal impurity level ($< 5\,mg\,kg^{-1}$) in the samples [47]. The source of the hydrogen is postulated [47] to be a cation vacancy compensated by two OH^- ions, an arrangement which has been shown [49] to be energetically favourable for the formation of atomic hydrogen. A corollary is, however, that atomic oxygen should accompany the hydrogen formation [47], this oxygen then possibly diffusing to form essentially a triple cluster of O^- ions located on a (1 1 1) surface plane. This arrangement, the V_1 paramagnetic centre [50], is catalytically active. A further consequence of this model is that the MgO becomes nonstoichiometric (cation deficient) and thus a p-type semiconductor. This factor can dramatically affect the sintering behaviour of the material, since this is controlled by the transport of material in the form of ions, and a change in stoichiometry or in the defect concentration, changes the number of possible paths for ion transport [51]. Ready [52] has shown that impurities which produce an increase in the vacancy concentration in the sub-lattice containing the ions whose movement is rate determining for the sintering (in MgO the O^{2-} ions) increase the densification rate. In MgO, this increase would, however, only be up to the point where the decreasing vacancy concentration in the Mg^{2+} sub-lattice causes reduced sintering by limiting this ion's diffusion possibilities.

3.3. The kinetics of the decomposition reaction

The kinetics of the dehydroxylation reaction have been studied, mainly using differential thermal analysis (DTA) or (differential) thermogravimetry [(D)TG], by a large number of workers. In a recent review article, Sharp [53] concluded, however, that many of the methods developed for the kinetic analysis of DTA traces of solid state reactions yield unreliable values for the activation energy and order of reaction. He also concluded that the kinetics were strongly dependent on the ambient water vapour pressure and that, under vacuum, the activation energy (E) is about $84\,kJ\,mol^{-1}$, which is similar to the enthalpy of the reaction as quoted by Giauque and Archibald [54, 55] in the standard works on the reaction thermodynamics of this system. Since Sharp's article was published, most analyses have concentrated on the use of thermogravimetry, and recent workers [56, 57] have confirmed the above value under these conditions. Chen and Fong [58], who allowed $Mg(OH)_2$ to decompose in a semi-sealed system, and Kanungo [59, 60], who decomposed large samples in air, obtained much higher values for the activation energy; 210 to 350 $kJ\,mol^{-1}$ (mean $222\,kJ\,mol^{-1}$) and 188 to $225\,kJ\,mol^{-1}$, respectively. Bouvier *et al.* [61], who carried out TG analyses of the decomposition of natural brucite and seawater precipitated $Mg(OH)_2$ in air, obtained a value for the brucite of $274\,kJ\,mol^{-1}$ and for the $Mg(OH)_2$ of $356\,kJ\,mol^{-1}$. The decomposition rate constant was shown to be dependent on the reciprocal of the square of the particle size of the material.

This wide difference between E values determined in vacuum and in air can be explained by

postulating that the limiting step in the decomposition is the diffusion of evolved water away from its formation site, this being very likely to show the type of pressure dependence noted. Garn and Freund [44] concluded that the decomposition is unlikely to be explainable by any extant kinetic equation (except fortuitously), since these do not include terms describing such pressure dependence. Despite this, a number of workers [57, 61, 62] have assumed particular reaction equations for the purposes of calculation, a procedure which is only justified since Sharp [53] has shown it to have little effect on calculated values of activation energy.

4. Factors affecting the properties of the product MgO

The properties of the MgO formed by the decomposition of $Mg(OH)_2$ depend on the conditions under which the decomposition occurs, on the heat treatment to which the MgO is subject after decomposition, and on the physico-chemical properties of the precursor. For example, MgO powder prepared by thermal decomposition between 300° C and 400° C has a higher heat capacity [63], a higher heat of solution [28, 64] and higher rates of dissolution in acid [65] and rehydration in water [66–68] than "bulk" MgO. The higher values indicate that MgO prepared at low temperatures is "active" or "caustic", and of higher energy content than bulk (equilibrated) material. This higher energy content may be due to the powder having a higher specific surface area, or to the existence of strain energy in the lattice (see previous section), or to both.

Further heat treatment of the MgO formed results in growth of the minute crystals by material transport (primarily surface diffusion because of the low temperature) and sintering together of the crystals. The extent to which these phenomena influence the properties of the MgO powder is determined by the temperature, the time, and the atmosphere surrounding the crystals. The water content of the atmosphere is extremely important in this latter regard. The various factors and their influence are examined in detail below.

4.1. Absolute pressure and water vapour partial pressure during calcination

Decomposition of $Mg(OH)_2$ under vacuum allows the rapid removal of evolved water vapour from the crystals and prevents the outward diffusion of the water becoming the rate determining step for the process. If the pressure of (dry) gas surrounding the decomposing crystals is increased the rate of reaction is slowed as a result of hindered diffusion down the lowered pressure gradient (created by the evolution of water), despite the fact that the ambient gas is not saturated with water [44].

The presence of water molecules in the system, whether they are evolved from the $Mg(OH)_2$ on reaction, or are inserted into the system during processing (e.g. into the gas stream via decomposition products from gas burners), strongly influences both the nucleation and growth kinetics of the product MgO. The water molecules appear to enhance nucleation of the product [69], giving MgO crystals of a smaller size than those resulting from vacuum treatment at the same temperature. The MgO thus has a higher surface and reactivity owing to its smaller crystal size [16, 41]. On further heat treatment of the product, the water molecules present collide and interact with the MgO surface according to the following postulated reaction mechanism [70, 71]:

$$Mg^{2+} + O^{2-} + H_2O\downarrow \rightarrow Mg^{2+} + 2OH^- + V_m \rightarrow Mg^{2+} + O^{2-} + H_2O\uparrow \rightarrow V_m + V_o \qquad (2)$$

where V_m indicates a cation vacancy and V_o an anion vacancy. This mechanism, as well as changing the vacancy concentration and thus the possibilities for material transport [51, 52], also provides a possible direct contribution to O^{2-} ion movement by desorption of oxygen to form water from a site adjacent to that on which it was originally adsorbed [70]. Such adsorption/desorption gives rise to rapid crystal growth and agglomeration with concomitant reductions in surface area and reactivity of the product MgO, particularly as the temperature is increased. This temperature dependence derives from the relationship describing the residence time (t) of an adsorbed water molecule at the surface:

$$t = t_0 \exp(Q/RT) \qquad (3)$$

where, Q is the heat of adsorption (80 to 160 kJ mol^{-1}) [70], and t_0 the time of vibration of the adsorbed molecule (10^{-13} sec) [72], i.e. the exchange time for adsorbed water molecules decreases with increasing temperature.

The kinetics of crystal growth in the presence of water vapour have been found [73], in the

temperature range 435 to 790° C, to follow the rate equation:

$$G^n = kt \quad (4)$$

where G is the crystal size, k is a constant, t is the time and n is a constant (5 to 7). The activation energy was determined as $130 \pm 12\,kJ\,mol^{-1}$, i.e. lower than the accepted values for bulk diffusion [74, 75] ($330\,kJ\,mol^{-1}$ for Mg^{2+} in MgO and $261\,kJ\,mol^{-1}$ for O^{2-} in MgO), or for surface diffusion [76] in MgO ($376\,kJ\,mol^{-1}$). Enhanced surface diffusion was postulated as the operative mechanism. A limiting value of partial pressure of water ($266\,Nm^{-2}$) below which no enhanced crystal growth occurred was noted by Faure and Imelik [77]. Riddell [78] noted that the crystal growth rate at partial pressures of water above $610\,Nm^{-2}$ (Eastman [79] $660\,Nm^{-2}$) was proportional to $(P_{H_2O})^{1.0}$, but that at a pressure of $0.075\,Nm^{-2}$ a lower dependence was indicated. A similar break in the rate of shrinkage of compacts of MgO at low water vapour pressures was noted by Hamano *et al.* [71]. Such a break may indicate the pressure at which monolayer coverage of the MgO surface by adsorbed water molecules becomes incomplete.

It is perhaps worth mentioning here that this enhanced crystal growth in the presence of water vapour also occurs during the sintering of compacts of the MgO product to form 'dead-burned' material, i.e. the final stage in the production of refractory grade MgO. Enhanced initial and intermediate stage sintering (i.e. stages of sintering where pores in the compact remain open and accessible to such gaseous influence factors) was originally noted by Eubank [80] and has since been confirmed by numerous other workers [28, 70, 71, 79, 81–84]. Most report a strong enhancement of sintering in the presence of water vapour, although one [83] reports retarded densification and another [70] draws attention to the fact that retardation may occur. Whether water vapour enhances or retards densification is probably strongly dependent on other characteristics of the material (e.g., chemical composition) which will be discussed in the following sections of this paper. Such factors may be expected to control the speed of movement of the crystal surfaces (in refractory terminology the grain boundaries) and whether the pores present in the compact remain attached to the grain boundaries during sintering, which renders densification easier, or break away from the boundary, which makes their removal more difficult. For a fuller discussion of pore/grain boundary relationships in the above sense during sintering, articles by Brook [85–87], White [88, 89], Hsueh *et al.* [90] and Spears and Evans [91] are recommended.

4.2. Temperature and time of calcination

The rapidity of crystal growth and sintering of the MgO formed by decomposition is, to a large measure, controlled by the temperature and time of heat treatment. Crystal (grain) growth kinetics, as stated previously, have been shown [75, 78] to fit an equation of the form:

$$G^n - G_o^n = kt = A \exp\left(-\frac{E}{RT}\right) \cdot t \quad (5)$$

where, G and G_o are the (X-ray) crystal sizes at times t and zero, and n is a constant between 5 and 7. This relationship holds until the crystal size reaches 50 to 67 nm [78]. Above this size there is an apparent mechanism change and the crystal growth kinetics have been found [89] to fit the equation:

$$dG/dt = M_b\left(\frac{A}{G} - c\right) \quad (6)$$

where, A and c are constants and M_b is the grain boundary mobility (which will be constant for a particular temperature and impurity content). This equation has the form expected if crystal growth was occurring by the migration of grain boundaries past stationary pores, assuming that the rate of grain growth could be identified with the rate of grain boundary migration. The change in kinetics generally occurred when the density had reached 90 to 95% of its theoretical value. Activation energies for grain growth were calculated as about $108\,kJ\,mol^{-1}$ below about 1200° C and $335\,kJ\,mol^{-1}$ above about 1200° C. The latter value, without identifying mechanism, seems reasonable and agrees with the calculated energy [75] for intrinsic diffusion of Mg^{2+} ions in MgO. The former value is of the same order as that calculated by Aihara [73], where the mechanism attributed was enhanced surface diffusion.

These observations have implications for the calcining of $Mg(OH)_2$ to produce an MgO with specific crystal size, and hence activity and surface area, since these are closely related to the crystal size. If we consider the region below 1200° C

(the temperature range normally used in the commercial production of caustic MgO), the substitution of values for temperature and time into Equation 5 gives the values shown in Table I for crystal growth.

These observations have implications for the temperature are important for the achievement of a particular crystal size in the product. In the 500 to 700° C range, an increase in calcining temperature of about 6° C has the same effect as increasing the residence time of the material at that temperature by 1 min. In the 700 to 900° C range, an increase of about 9° C gives an effect equivalent to an additional 1 min residence. These values are valid for high purity materials calcined in the presence of water, but do not take into account additional effects on crystal growth and sintering caused by, for example, changes in precursor impurity content or morphology.

4.3. $Mg(OH)_2$ morphology

The MgO formed by the thermal decomposition of $Mg(OH)_2$ (and other magnesium salts [8, 10, 27, 40, 80, 92, 93]) retains, on a microscopic scale, the crystal shape of the precursor. The form of the precursor crystal is given by the "relics" or "pseudomorphs". They consist of minute crystals of cubic MgO attached along their edges/corners to form a larger crystal aggregate defining the precursor crystal. This is shown in Fig. 3.

For precursor crystals more than about 6 nm thick, multiple layers of MgO crystals have been reported to be present in the pseudomorph [29]; below this thickness only single layers have been observed. The formation of multiple layers about 6 nm thick, stacked along the *c*-axis of the original $Mg(OH)_2$ crystal, can be attributed to strain cracking in the plane perpendicular to this axis (this plane contains OH^- ions in adjacent layers which diffuse out to give water and form the 'weak link' in the structure, see Fig. 2.)

The formation of these highly orientated layers of MgO from thick $Mg(OH)_2$ crystals has been put forward [11, 95] as a possible explanation for the formation of a duplex microstructure in deadburned MgO derived from $Mg(OH)_2$. This type of microstructure consists of a few large grains of MgO, presumably formed from well orientated crystal layers, surrounded by a large number of smaller grains formed from less well orientated layers. An alternative form of this type of microstructure is large (up to millimetre dimensions) polycrystalline particles of high density surrounded by a porous matrix of small grains. It is thought that this latter phenomenon occurs because the plate-like $Mg(OH)_2$ crystals have a strong tendency to orientate themselves face to face during thickening/washing etc and thus give large multiple layer pseudomorphic aggregates, e.g. during calcining. The orientation of the multiple layers of MgO crystals may be conducive to enhanced sintering within such pseudomorphs, and to the formation of quite large strong particles (possibly the 'gritty' particles often noted in commercially calcined caustic MgO), which may pass through subsequent compaction (briquetting) operations into the deadburned product. Such microstructures are not noted in deadburned MgO produced from precursors where the decomposition does not occur topotactically (e.g. $MgCO_3$, MgC_2O_4, $MgSO_4$, etc.). In the latter materials, the rate of crystal growth will be more influenced by the bulk impurity and defect concentrations in the MgO crystals than in MgO derived from $Mg(OH)_2$, where an additional contribution owing to the high preferred orientation of the multiple layers will be present.

The morphology (particularly thickness) of the $Mg(OH)_2$ crystals, as well as the bulk impurity and defect concentrations in and adsorbed impurity levels on the crystals, have been shown [29, 95–98] to be controlled by the conditions (pH, temperature, solute concentrations) present during their precipitation and subsequent ageing in an

TABLE I Effect of calcining temperature and time on the crystal size of MgO

Temperature (° C)	Crystal size,* after	
	5 min	20 min
500	$(1.02–1.34)G_o$	$(1.1–1.54)G_o$
700	$(1.46–2.16)G_o$	$(1.88–2.64)G_o$
900	$(2.22–3.0)G_o$	$(2.92–3.66)G_o$

*Original crystal size = G_o.

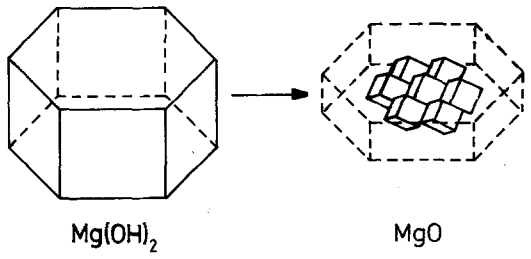

Figure 3 Precursor–product pseudomorphic relationships in $Mg(OH)_2$ and MgO (after Guilliat and Brett [94]).

aqueous environment. However, owing to the above mentioned tendency for the $Mg(OH)_2$ crystal platelets to stack face to face, calcining under commercial conditions is likely to result in the creation of a proportion of orientated pseudomorphs which may give rise to duplex microstructures in sintered products whatever the size of the $Mg(OH)_2$ crystals. Breakdown of the stacked platelets by mechanical treatment prior to calcining may enable the production of agglomerates with a smaller, or at least more localized degree of face to face orientation, and might partially explain recently reported Japanese successes [99] in increasing the sinterability of $Mg(OH)_2$ and MgO by milling, although the effect of the reduction in particle size will also play a major role.

4.4. Impurities in the MgO

While both bulk and adsorbed impurities in the $Mg(OH)_2$ are not thought to strongly influence the thermal decomposition reaction as such, they are known to influence the course of sintering and grain growth during further thermal treatment. The exact influence which the impurities have depends on the nature of the impurity, its location (bulk or adsorbed), and on possible interactions with other impurities. A summary of cationic impurities which have been found to influence the densification of MgO has been presented by Hamano [100] and is reproduced in Table II.

4.4.1. CaO

Ca^{2+} ions, which have an ionic radius of 0.099 nm, should be able to replace Mg^{2+} ions (radius 0.066 nm) in MgO, although quite large strains will be induced in the crystal lattice. Reasonably high solid solution of CaO in MgO is observed. No effect on the defect concentration in the crystal is to be expected.

The extent of solid solution of CaO in MgO increases with temperature [101], but at normal calcining temperatures (about 900° C) is probably < 0.5 wt% [102]. CaO, when present at levels above the solid solution limit appropriate for the temperature, has been shown [102] to enhance densification during deadburning, possibly by

TABLE II Metal oxide impurities and their effects on the densification of MgO (taken from [100], ionic radii quoted from [128]). + indicates a positive effect on densification, − a negative one. Where both symbols are shown, the effect is dependent on impurity content

Impurity	Valency	Solid solution*	Ionic radius (nm)	Sintering temperature (° C)				
				1225–1720	1700–1800	1300–1500	1500–1600	1300
MgO	+ 2		0.066					
Li_2O	+ 1	l (?)	0.068	+	+ (−)			+
Na_2O	+ 1		0.097	−				
CuO	+ 2		0.072	+				
BeO	+ 2	e	0.035				+	+
CaO	+ 2	l	0.099	−	−	+		
BaO	+ 2		0.134	−				
CdO	+ 2		0.097		−			
ZnO	+ 2		0.074		−		+	
FeO	+ 2	e	0.074	+	+			
NiO	+ 2	e	0.069		−			+
CoO	+ 2	e	0.072		−			
PbO	+ 2		0.120		−			
B_2O_3	+ 3		0.023					+
Al_2O_3	+ 3	l	0.051	+ (−)	−	+		+
Fe_2O_3	+ 3	l	0.064	+	+	+		+
Cr_2O_3	+ 3	e	0.063	+ (−)	−			+
Mn_2O_3	+ 3	e	0.066					
SiO_2	+ 4	l	0.042	+ (−)	+ (−)	+		+(−)
TiO_2	+ 4	l	0.068	+	+	+		+
ZrO_2	+ 4	l	0.079	+	+			
MnO_2	+ 4	l	0.060	+	+			
V_2O_5	+ 5	l	0.059	+	+		+	

*l = limited solution.
e = extensive solution.

slowing the movement of grain boundaries and thus preventing the engulfment of pores. CaO below the solubility limit has also been shown [103, 104] to preferentially segregate into the grain boundary, where it may also be expected to influence grain growth kinetics. Little effect on crystal growth during calcination was noted [105] due to the presence of $Ca(OH)_2$, $CaCO_3$ or CaC_2O_4 in the $Mg(OH)_2$. A very strong effect was, however, noted with other calcium salts, and crystal growth on calcining was remarkably enhanced by the presence of $CaCl_2$ [105]. Gorin and Metzer [106] also report a linear decrease in reactivity as a function of $CaCl_2$ content. This effect is probably due to the presence of Cl^- ions rather than Ca^{2+} ions (see Section 4.4.9).

4.4.2. SiO_2

Si^{4+} ions, with their small size (0.042 nm), should be easily able to replace Mg^{2+} ions in the MgO crystal lattice, although they will introduce quite major lattice strains.

Solution only occurs to very low levels owing to such strains, and to differences in the electropositivity of the two ions and, in fact, SiO_2 appears to show retrograde solubility in MgO at high temperatures [107]. The SiO_2 solubility limit at about 900° C is probably only about 0.02 wt %, but this is sufficient to change the defect concentrations in the material quite dramatically. If the Si^{4+} ions replaced Mg^{2+} ions in the lattice, the material would become cation deficient and the grain growth/sintering would be expected to be retarded, since the rate determining step in the sintering of MgO is the transport of O^{2-} ions. Hamano *et al.* [108] note that the presence of SiO_2 at above the 0.3 wt % level retarded deadburning shrinkage and below this level a slight enhancement of shrinkage (above that of pure MgO) occurred. Layden and McQuarrie [109], and Nelson and Cutler [110] also noted a similar effect. These unexpected results may indicate that Si^{4+} ions enter the MgO lattice as interstitial cations and give rise to a strained lattice with cation excess (equivalent in effect to anion vacancies).

4.4.3. Iron oxides

Fe^{2+} ions may be expected to isomorphically replace Mg^{2+} ions without affecting the vacancy concentration. However, as the temperature or partial pressure of oxygen increase, the Fe^{3+} ions formed [111–113] may give rise to oxygen interstitials or, more likely [113], cation vacancies in the material. FeO is completely soluble in MgO (the two form an isomorphous series) but the solubility of Fe_2O_3 in MgO at temperatures below 1000° C does not appear to have been exactly established. At 1200° C in air, the solubility has been given [114] as about 10 wt %, and at 1400° C about 35 wt %.

The presence of iron in MgO has been shown to enhance the sintering [108, 110, 115] and grain growth [114, 116] in the material even at very low levels [108]. This result is probably due to the enhanced O^{2-} ion flux required to maintain electrical neutrality during the Fe^{2+}/Fe^{3+} transition.

4.4.4. B_2O_3

The B^{3+} ion, because of the large difference in its size and that of the Mg^{2+} ion, does not replace the latter in its compounds. No solid solution of B_2O_3 in the MgO is observed [117]. Instead, the separate phase $3MgO.B_2O_3$ is formed at B_2O_3 contents up to about 37 wt %, and other phases are formed at higher B_2O_3 contents. In the presence of CaO as an impurity in the MgO, preferential formation of calcium borates possibly occurs [118, 119].

B_2O_3 has been shown to have a positive effect on grain growth and sintering [117, 120], even at temperatures as low as 1050° C, while evaporation of B_2O_3 from pure MgO (no CaO present) has been observed above about 750° C [117].

4.4.5. Al_2O_3

Al_2O_3 has been reported to both positively [109, 115] and negatively [110] affect the sintering of MgO, depending on the level of Al_2O_3 present. In that the solubility of Al_2O_3 in MgO is lower than that of Fe_2O_3 at all temperatures, the solubility limit will be more rapidly reached, and phase separation of $MgAl_2O_4$ spinel is to be expected. This appears to detrimentally affect grain boundary movement characteristics. At levels below the solubility limit, effects similar to those caused by Fe_2O_3 are to be expected (i.e., a reduction in grain growth/sintering caused by cation vacancies). The reported positive effects of Al_2O_3 on sintering are likely to be due to reactions with other impurities to form a liquid phase [115], or to a form of reaction sintering by impurity segregation to the grain boundaries [109].

4.4.6. Chromium oxides

Ikegami *et al.* [121] note that the presence of chromium ions in the $Mg(OH)_2$ before calcining leads to inappreciable differences in the particle shape and size of the MgO produced by calcination. The MgO did, however, appear to have a narrower size distribution in the presence of chromium ions.

Sintering and densification on deadburning is reported to be enhanced by the presence of chromium ions when sintering is carried out under vacuum [101, 121], but retarded under more normal (oxidizing) regimes [109]. The valency of the chromium ion shows a dependence on the oxygen partial pressure and temperature, in a similar way to that of iron [122]. This variation may be expected to give rise to an optimum oxygen partial pressure for the sintering of chromium-doped MgO at a particular temperature [119] in order to maximize the material transport possibilities.

4.7.7. Manganese oxides

Mn^{2+} and Mn^{3+} ions are soluble in MgO, whereas Mn^{4+} ions appear to segregate to the crystal surfaces [123] and react to give Mg_6MnO_8. Mn^{2+} ions are only stable in reducing atmospheres, whereas the other two forms show a similar temperature/oxygen partial pressure dependence to iron and chromium ions. Under oxidizing conditions at temperatures above 800° C, the higher valency forms are more stable and give rise to defect concentration changes and grain boundary segregation effects which affect the crystal growth kinetics of the MgO formed on caustic calcination [123]. A coarser MgO product results.

4.4.8. Alkali metal oxides

Of the alkali metal impurities considered here (lithium, sodium and potassium) only Li^+ is expected to show any significant substitution for Mg^{2+} ions in MgO because of the limitations imposed by differences in ionic radii. Such substitution would have the effect of making the material anion deficient, or of balancing the charge differences introduced by impurities of valency higher than two, without the formation of the normally associated cation vacancies. This latter effect might be expected to slow grain growth and sintering in the calcine and, in fact, Guilliat and Brett [123] report that crystal growth in MgO doped with both manganese and lithium is slower than growth seen after doping with manganese alone. Quantification of the effect proved impossible because of volatilization of lithium from the MgO [124]. The formation of anion vacancies in MgO would be expected to cause enhanced sintering (although this would only be important for very high purity materials, i.e. without cation vacancies), and lithium compounds have been reported [109, 110, 125, 126] to enhance the sintering of high purity MgO during deadburning. However, the compounds added were halides, sulphates, carbonates, nitrates, etc., and the sintering could have been further enhanced by effects due to the associated anion (variations in fired density were certainly noted [125] which may be attributable to such a cause). This will thus be further discussed in Sections 4.4.9 and 4.4.10.

Na^+ and K^+ ions are too large to replace Mg^{2+} ions in the lattice, but can certainly be adsorbed on the crystal surfaces of $Mg(OH)_2$ formed by precipitation from solutions containing their salts. On calcination, the presence of Na^+ ions has been reported [29] to reduce the surface area of the caustic MgO formed, implying that its presence enhances grain growth and sintering. However, other workers report that additions of NaOH to $Mg(OH)_2$ filtercake give rise to a higher surface area in the product MgO [127], implying reduced grain growth/sintering. This agrees with Layden and McQuarrie [109] who report a detrimental effect on densification during deadburning.

4.4.9. Halides

As noted in Section 4.4.1, the presence of Cl^- ions strongly enhances grain growth of the product MgO [106]. The crystal structures of $Mg(OH)_2$ and $MgCl_2$ are identical, and Cl^- ions can isomorphically replace OH^- ions in the lattice. $MgCl_2$, however, is reported [128] to melt at 714° C and boil at 1412° C without dissociation, so that at normal calcining temperatures (800 to 1000° C) it probably enhances grain growth and sintering by forming a liquid phase in which ion transport is enhanced. A similar mechanism (i.e. liquid phase sintering) is probably responsible for the enhanced sintering given [109, 124] by additions of lithium halides. The presence of chlorine gas in the furnace atmosphere has been reported [83] to enhance densification during low temperature (1100° C) deadburning experiments. Liquid phase sintering is again the probable explanation.

The presence of F^- ions would be expected only to influence crystal growth in MgO at higher temperatures (MgF_2 is tentatively reported [128] to melt at 1266° C), if the above mechanism were the cause of enhancement. Ikegami *et al.* [129] have confirmed such a high temperature effect, while Hodge [130] has reported enhanced grain growth and creep due to the concentration of residual F^- at MgO grain boundaries in sintered compacts.

The presence of Br^- and I^- ions should lead to enhanced low temperature liquid phase sintering, although MgI_2 decomposes at $<637°$ C [128] and thus presumably results only in a negligible contribution to sintering at normal calcining and deadburning temperatures.

4.4.10. Other impurities

4.4.10.1. Cationic impurities. A number of other cations may be expected to influence the sintering and grain growth of MgO. Three, at least, have been found to be particularly effective, i.e. Ti^{4+}, Zr^{4+} and V^{5+}. All might be expected to give rise to cation vacancies due to their higher valencies and thus to retard sintering, but exactly the opposite has been found to be the case [100, 109, 110, 115, 126, 131], i.e. sintering is dramatically enhanced. For V^{5+} this has been explained by the presence of a liquid phase [109]. For Zr^{4+}, Reijnen [126] has proposed that a shift of O^{2-} ions towards the highly charged Zr^{4+} ions increases the electrostatic energy, thus favouring the formation of an extra vacancy pair to allow incorporation of the larger cation in the magnesium sub-lattice. This should give rise to an enhanced O^{2-} ion mobility and sintering. A similar effect, in smaller degree due to the smaller size of the Ti^{4+} ion, can presumably be expected for a TiO_2 impurity. This strongly enhanced sintering with ZrO_2 has been found to take place only at contents up to the solubility limit of the material in MgO (0.21 wt % for ZrO_2 at 1650° C) and only if the ZrO_2 was incorporated in MgO by a wet chemical process, e.g. coprecipitation of $Zr(OH)_2$ and $Mg(OH)_2$ [126, 132]. An explanation of this latter phenomena may be that other methods of incorporation (e.g. co-milling) result in localized concentrations of ZrO_2 in excess of the amount soluble in MgO, and these give rise to hindered sintering by blocking grain boundary movement.

4.4.10.2. Anionic impurities. Little work appears to have been carried out on the influence of anionic impurities other than the halides in MgO. Leipold and Kapadia [133] report that the SO_3^{2-} ion has a more detrimental effect on the densification of MgO during hot pressing than Cl^-, F^- and OH^- ions. This was attributed to species volatility. Gregg and Packer [134] report that additions of sulphate to precipitated $Mg(OH)_2$ before calcination result in a maximum surface area in the product MgO being produced at a higher temperature than that for pure MgO, i.e. sintering was apparently reduced. Rhodes *et al.* [10] report that the presence of $MgSO_4$, which decomposes above 1300° C, gives rise to the formation of $CaSO_4$, in calcium-containing MgO. Hamano [81] notes that MgO formed from $MgSO_4$ and $Mg(NO_3)_2$ gave rise to products which showed a low densification tendency.

5. Conclusions

A critical evaluation of literature results leads to the following conclusions on the processes occurring during the calcination of $Mg(OH)_2$ to MgO. The thermal decomposition of $Mg(OH)_2$ to MgO, which commences below 300° C, occurs topotactically by a mechanism involving the formation of a defect layer of $Mg(OH)_2$ structure but contracted unit cell dimensions. This structure recrystallizes suddenly to the cubic structure characteristic of MgO. Recrystallization will, if the $Mg(OH)_2$ particles are larger than about 60 nm, give rise to cracking of the product MgO into particles of about 5 to 10 nm as the lattice fracture stress is exceeded by the contractional strains. The activation energy of the reaction is about 84 kJ mol^{-1} in vacuum, but may be >350 kJ mol^{-1} in air owing to the trapping of evolved water at its formation site in thicker beds of material, i.e. the reaction kinetics are dependent on both absolute and partial water vapour pressure.

The presence of water at the reaction site leads to enhanced nucleation of MgO and thus to a finer crystal size in the product MgO. The continued presence of water molecules on, or in close proximity to, the MgO surface at temperatures above that of decomposition leads to enhanced crystal growth and agglomeration by increased surface diffusion. The kinetics of crystal growth in the temperature range 435 to 790° C, and up to a crystal size of about 70 nm, follow the rate equation:

$$G^n = kt = A \exp\left(-\frac{E}{RT}\right) \cdot t, \qquad (7)$$

where G is the crystal size at time t, n is a constant (5 to 7), and E is the activation energy. Above about 70 nm, the mechanism apparently changes such that the rate of grain (crystal) growth is linked to the rate of migration of grain boundaries which may or may not contain pores. Activation energies for grain growth appear to be about 110 to 130 kJ mol^{-1} below 1200° C, and 335 kJ mol^{-1} above 1200° C. From the equation above, a simultaneous dependence of crystal size on both calcining temperature (T) and residence time (t) at temperature is indicated.

The morphology (particularly the thickness or degree of stacking) of the $Mg(OH)_2$ precursor crystals has been shown to be a possible factor in the formation of well oriented layers of MgO crystals which rapidly sinter together and densify as a unit. The conditions during precipitation and subsequent ageing of the $Mg(OH)_2$ crystals control their morphology. The degree of stacking may be influenced by mechanical treatment of the slurry before calcining.

Impurities in the $Mg(OH)_2$ which positively influence MgO crystal growth during low temperature calcining are Fe^{2+}, Fe^{3+}, Si^{4+}, Cl^-, Li^+, Mn^{3+}, Mn^{4+} and possibly B^{3+}, V^{5+}, Zr^{4+} and Ti^{4+}. Those which appear to have little effect are Ca^{2+}, Cr^{3+}, F^-, and possibly Al^{3+}, and those which negatively influence crystal growth are Na^+, K^+, SO_3^{2-}, and possibly NO_3^- and NO_2^-.

Owing to the large number of factors which influence the properties of the product MgO, any research in this area must involve a high experimental effort in precursor, processing and product characterisation if understanding of the calcining process and the products resulting is to lead to improvements of either the process used in, or the products deriving from, commercial magnesia plants. Such comprehensive studies do not appear to have been carried out to date, but could be expected to be extremely fruitful in terms of improved processing methods to give caustic magnesias with particular properties.

Acknowledgements

The author wishes to thank the directors of Billiton Research BV and Shell International Research Maatschappij for permission to publish this paper.

References

1. N. H. BRETT, K. J. D. MACKENZIE and J. H. SHARP, *Quart. Rev. Chem. Soc.* **24** (1970) 185.
2. R. D. SHANNON and R. C. ROSSI, *Nature* **202** (1964) 1000.
3. M. C. BALL and H. F. W. TAYLOR, *Min. Mag.* **32** (1961) 754.
4. J. BERNAL, *Trans. Faraday Soc.* **34** (1938) 834.
5. N. H. BRETT, *Min. Mag.* **37** (1969) 244.
6. J. DEQUENNE and C. PACQUE, *Bull. Soc. Fr. Ceram.* (1973) 69.
7. F. FREUND, *Ber. deut. keram. Ges.* **47** (1970) 739.
8. A. F. MOODIE, C. E. WARBLE and L. S. WILLIAMS, *J. Amer. Ceram. Soc.* **49** (1966) 676.
9. R. PAMPUCH, Z. LIBRANT and J. PIEKARCZYK, *Phys. Sintering* **5** (1973) 263.
10. W. H. RHODES, B. J. WUENSCH and Th. VASILOS, NTIS AD-760017, March 1973.
11. W. H. RHODES and B. J. WUENSCH, *J. Amer. Ceram. Soc.* **56** (1973) 495.
12. T. A. WHEAT and T. G. CARRUTHERS, "Science of Ceramics IV" (Academic Press, London, 1968) p. 33.
13. W. R. EUBANK, *J. Amer. Ceram. Soc.* **34** (1951) 225.
14. R. M. DELL and S. W. WELLER, *Trans. Faraday Soc.* **55** (1959) 2203.
15. J. F. GOODMAN, *Proc. Royal Soc.* **247** (1958) 346.
16. P. J. ANDERSON and R. F. HORLOCK, *Trans. Faraday Soc.* **58** (1962) 1993.
17. J. W. NIEPCE and G. WATELLE, *J. Phys. Colloq.* (1977) 365.
18. J. W. NIEPCE, G. WATELLE and N. H. BRETT, *J. Chem. Soc.* **74** (1978) 1530.
19. G. W. BRINDLEY, in "Progress in Ceramic Science" (Pergamon, London, 1963) pp. 7–9.
20. A. CIMINO, P. PORTA and M. VALIGI, *J. Amer. Ceram. Soc.* **49** (1966) 152.
21. F. FREUND, *Ber. deut. keram. Ges.* **52** (1975) 53.
22. Z. LIBRANT and R. PAMPUCH, *J. Amer. Ceram. Soc.* **51** (1968) 109.
23. F. FREUND and V. SPERLING, *Mater. Res. Bull.* **11** (1976) 621.
24. F. FREUND, R. MARTENS and N. SCHEIKH-OL-ESLAMI, *J. Therm. Anal.* **8** (1975) 525.
25. N. G. KAKAZEI, *Sov. Powder Metall.* **19** (1974) 84.
26. R. MARTENS, H. GENTSCH and F. FREUND, *J. Catal.* **44** (1976) 366.
27. S. IWAI, H. MORIKAWA, T. WATANABE and H. AOKI, *J. Amer. Ceram. Soc.* **53** (1970) 335.
28. D. T. LIVEY, B. M. WANKLYN, M. HEWITT and P. MURRAY, *Trans. Brit. Ceram. Soc.* **56** (1957) 217.
29. V. A. PHILLIPS, H. OPPERHAUSER and J. L. KOLBE, *J. Amer. Ceram. Soc.* **61** (1978) 75.
30. N. H. BRETT and P. J. ANDERSON, *Trans. Faraday Soc.* **63** (1967) 2044.
31. R. R. BALMBRA, J. S. CLUNIE and J. F. GOODMAN, *Nature* **209** (1966) 1088.
32. R. S. GORDON and W. D. KINGERY, *J. Amer. Ceram. Soc.* **49** (1966) 654.

33. Idem, *ibid.* **50** (1967) 8.
34. R. PAMPUCH, in Proceedings of the 9th Conference on the Silicate Industry, Budapest, 1967, (Pub. 1968) p. 143.
35. I. F. GUILLIATT and N. H. BRETT, *Trans. Brit. Ceram. Soc.* **69** (1970) 1.
36. D. C. GARN, B. KAWALEC and J. C. CHANG, *Thermochim. Acta* **26** (1978) 375.
37. K. LØNVIK, *ibid.* **27** (1978) 27.
38. R. PAMPUCH and Z. LIBRANT, *Zesz. Nauk. Akad. Gorn.-Hutn. Cracow Ceram.* **11** (1969) 45.
39. K. HAMANO and Y. AKIYAMA, *Bull. Tokyo Inst. Technol.* **103** (1971) 1.
40. K. D. OH, H. MORIKAWA, S. IWAI and H. AOKI, *Yogyo Kyokai Shi* **82** (1974) 442.
41. S. I. KONTOROVICH, L. M. SHISHLYANIKOWA, V. V. DAVYDOV and E. D. SHCHUKIN, *Izv. Akad. Nauk. SSSR Neorg. Mater.* **11** (1975) 187.
42. T. TOMIZAWA, H. HASHIMOTO and K. MOTEKI, *Kogyo Kogahu Zasshi* **69** (1966) 2263.
43. F. FREUND, *Ber. deut. keram. Ges.* **42** (1965) 23.
44. D. C. GARN and F. FREUND, *Trans. Brit. Ceram. Soc.* **74** (1975) 23.
45. H. NÄGERL and F. FREUND, *J. Therm. Anal.* **2** (1970) 387.
46. F. FREUND and H. GENTSCH, *Ber. deut. keram. Ges.* **44** (1967) 51.
47. F. FREUND, R. MARTENS and H. GENTSCH, *Sci. Ceram.* **9** (1977) 308.
48. K. J. D. MACKENZIE, *J. Inorg. Nucl. Chem.* **32** (1970) 3731.
49. E. G. DEROUANE, J. G. FRIPIAT and J. M. ANDRÉ, *Chem. Phys. Lett.* **28** (1974) 445.
50. M. BOUDART, A. J. DELBOUILLE, E. G. DEROUANE, V. INDOVINA and A. B. WALTERS, *J. Amer. Chem. Soc.* **94** (1972) 6622.
51. P. J. L. REIJNEN, "Problems in Non-stoichiometry" (Rabenau, North Holland, 1970) p. 219.
52. D. W. READY, *J. Amer. Ceram. Soc.* **49** (1966) 366.
53. J. H. SHARP, *Trans. Brit. Ceram. Soc.* **72** (1973) 21.
54. W. F. GIAUQUE and R. C. ARCHIBALD, *J. Amer. Chem. Soc.* **59** (1937) 561.
55. W. F. GIAUQUE, *ibid.* **71** (1949) 3192.
56. J. M. CRIADO and J. MORALES, *J. Therm. Anal.* **10** (1976) 103.
57. K. M. ABD EL-SALAAM, R. M. GABR and A. A. SAID, *Surf. Tech.* **9** (1979) 427.
58. D. T. Y. CHEN and P. H. FONG, *J. Therm. Anal.* **12** (1977) 5.
59. S. B. KANUNGO, *J. Indian Chem. Soc.* **52** (1975) 108.
60. Idem, *Indian J. Chem.* **13** (1975) 180.
61. A. BOUVIER, H. J. GRIESSER and G. W. HERZOG, *Radex Rundsch.* (1980) 231.
62. P. H. FONG and D. T. Y. CHEN, *Thermochim. Acta* **18** (1975) 273.
63. G. JURA and C. W. GARLAND, *J. Amer. Chem. Soc.* **74** (1952) 6033.
64. K. TAYLOR and L. S. WELLS, *J. Res. Nat. Bur. Stand.* **21** (1938) 133.
65. H. T. S. BRITTON, S. J. GREGG and G. W. WINSOR, *J. Appl. Chem.* **2** (1952) 693.
66. M. J. MEHTA and D. S. DATAR, *Salt Res. Ind.* **1** (1972) 11.
67. R. I. RAZOUK and R. Sh. MIKHAIL, *J. Phys. Chem.* **59** (1955) 636.
68. L. G. BERG, M. G. ALTYKIS and A. P. PIRMATOV, *Russ. Inorg. Chem.* **12** (1967) 921.
69. P. J. ANDERSON, R. F. HORLOCK and R. G. AVERY, *Proc. Brit. Ceram. Soc.* **3** (1965) 33.
70. P. J. ANDERSON and P. L. MORGAN, *Trans. Faraday Soc.* **60** (1964) 930.
71. K. HAMANO, K. ASANO, Y. AKIYAMA and Z. NAKAGAWA, Report of the Research Laboratories for Engineering Materials (Tokyo Institute of Technology, Tokyo 1979) p. 59.
72. DE BOER in "The Dynamical Character of Adsorption" (Oxford University Press, Oxford, 1953) Chap. 3.
73. K. AIHARA and A. C. D. CHAKLADER, *Acta Metal.* **23** (1975) 855.
74. Y. OISHI and W. D. KINGERY, *J. Chem. Phys.* **33** (1960) 905.
75. R. LINDNER and G. D. PARFITT, *ibid.* **26** (1957) 182.
76. W. M. ROBERTSON, in "Sintering and Related Phenomena" (Gordon and Breach, New York, 1967) p. 215.
77. M. FAURE and B. IMELIK, *Bul. Soc. Chim. Fr.* (1971) 761.
78. D. RIDDELL, PhD thesis, Sheffield University, 1972.
79. P. F. EASTMAN and I. B. CUTLER, *J. Amer. Ceram. Soc.* **49** (1966) 526.
80. W. R. EUBANK, *ibid.* **34** (1951) 225.
81. K. HAMANO, Report of the Research Laboratories for Engineering Materials (Tokyo Institute of Technology, Tokyo, 1979) p. 11.
82. V. FIGUSCH, M. HAVIAR and Z. PANEK, *Silikaty* **23** (1979) 143.
83. C. HYDE and W. H. DUCKWORTH, AD 266 735 US Government Research Report 37 (1962) 69.
84. Japanese Patent 56032-322.
85. R. J. BROOK, *J. Amer. Ceram. Soc.* **52** (1969) 339.
86. Idem, *ibid.* **52** (1969) 56.
87. Idem, *Klei en Keram.* **27** (1977) 62.
88. J. WHITE, *J. Aust. Ceram. Soc.* **9** (1973) 60.
89. Idem, *Glass and Ceram.* **23** (1976) 43.
90. C. H. HSUEH, A. G. EVANS and R. L. COBLE, *Acta Met.* **30** (1982) 1269.
91. M. A. SPEARS and A. G. EVANS, *ibid.* **30** (1982) 1282.
92. C. M. PATHAK and V. K. MOORTHY, *Trans. Indian Ceram. Soc.* **35** (1976) 89.
93. L. BACHMANN, *Radex-Rundsch.* (1957) 564.
94. I. F. GUILLIATT and N. H. BRETT, *Phil. Mag.* **21** (1970) 671.
95. M. COPPERTHWAITE and N. H. BRETT, *Sci. Ceram.* **8** (1976) 85.
96. V. A. PHILLIPS, J. L. KOLBE and H. OPPERHAUSER, in Proceedings of the 50th International Conference on Colloids and Surfaces, San Juan, 1976, Vol 4, edited by M. Kerker (Academic Press, New York) p. 169.

97. Idem, *J. Cryst. Growth* **41** (1977) 235.
98. Idem, *ibid.* **41** (1977) 228.
99. K. YAMAMOTO and K. UMEYA, *Amer. Ceram. Soc. Bull.* **60** (1981) 636.
100. K. HAMANO, Report of the Research Laboratories for Engineering Materials (Tokyo Institute of Technology, Tokyo, 1979) p. 1.
101. W. C. GILPIN and D. R. F. SPENCER, *Refract. J.* **47** (1972) 4.
102. R. C. DOMAN, J. B. BARR, R. N. McNALLY and A. M. ALPER, *J. Amer. Ceram. Soc.* **46** (1963) 313.
103. H. LEIPOLD, *ibid.* **49** (1966) 498.
104. Idem, *ibid.* **50** (1967) 628.
105. K. HAMANO, K. MUROYAMA, Z. NAKAGAWA and K. SAITO, *Yogyo-Kyokai-Shi* 87 (1979) 474.
106. Ch. GORIN and A. METZER, in "Ceramic Microstructures" (Westview Press, Colorado, 1977), p. 184.
107. M. H. LEIPOLD, in "Ceramic Microstructures" (Wiley, Chichester, 1968). p. 289.
108. K. HAMANO, K. YOSHINO and H. TOGASHI, *Yogyo-Kyokai-Shi* **74** (1966) 312.
109. G. K. LAYDEN and M. C. McQUARRIE, *J. Amer. Ceram. Soc.* **42** (1959) 89.
110. J. W. NELSON and I. B. CUTLER, *ibid.* **41** (1958) 406.
111. B. PHILLIPS, S. SOMIYA and A. MUAN, *ibid.* **44** (1961) 167.
112. D. WOODHOUSE and J. WHITE, *Trans. Brit. Ceram. Soc.* **54** (1955) 333.
113. P. REIJNEN, "Reactivity of Solids" (Elsevier, Amsterdam, 1965) p. 562.
114. J. WHITE, in "High Temperature Oxides" edited by A. M. Alper (Academic Press, New York, 1970) p. 89.
115. H. J. S. KRIEK, W. F. FORD and J. WHITE, *Trans. Brit. Ceram. Soc.* 58 (1959) 1.
116. G. C. NICHOLSON, *J. Amer. Ceram. Soc.* **49** (1966) 47.
117. S. MIYAGAWA, S. HIRANO and S. SOMIYA, *Yogyo-Kyokai-Shi* **80** (1972) 53.
118. M. I. TAYLOR, W. F. FORD and J. WHITE, *Trans. Brit. Ceram. Soc.* **68** (1969) 173.
119. Idem, *ibid.* **70** (1971) 51.
120. K. HAMANO and Y. AKIYAMA, *Bull. Tokyo Inst. Technol.* (1975) 59.
121. T. IKEGAMI, M. TSUTSUMI, S. MATSUDA and H. SUZUKI, *Yogyo-Kyokai-Shi* 88 (1980) 8.
122. H. U. ANDERSON, *J. Amer. Ceram. Soc.* **57** (1974) 34.
123. I. F. GUILLIAT and N. H. BRETT, *J. Chem. Soc. Faraday Trans.* **68** (1972) 429.
124. A. CIMINO, M. SCHIAVELLO and F. S. STONE, *Discuss. Faraday Soc.* **41** (1966) 350.
125. L. M. ATLAS, *J. Amer. Ceram. Soc.* **40** (1957) 196.
126. P. REIJNEN, *Mater. Sci. Res.* **13** (1980) 368.
127. US patent 3689218.
128. "Handbook of Chemistry and Physics" 55th edn (Chemical Rubber Company, Ohio, 1975).
129. T. IKEGAMI, S. MATSUDA and H. SUZUKI, *Yogyo-Kyokai-Shi* **86** (1978) 97.
130. J. D. HODGE and R. S. GORDON, *Ceramurgia* **4** (1978) 17.
131. S. SANO, S. KATO, E. ISHII and T. IGA, *Nogoya Kogyo Gijutsu Shikensho Hokuku* **14** (1965) 201.
132. J. GREEN, unpublished work carried out at the T. H. Aachen, 1975–77.
133. M. H. LEIPOLD and C. M. KAPADIA, *J. Amer. Ceram. Soc.* **56** (1973) 200.
134. S. J. GREGG and R. K. PACKER, *J. Chem. Soc.* (1955) 51.

Received 1 July
and accepted 16 July 1982